CrossMark

RESEARCH PAPER

Electrochemical sensor for rutin detection based on Au nanoparticle-loaded helical carbon nanotubes

Haitang Yang · Bingyue Li · Rongjing Cui · Ruimin Xing · Shanhu Liu

Abstract The key step in the fabrication of highly active electrochemical sensors is seeking multifunctional nanocomposites as electrode modified materials. In this study, the gold nanoparticle-decorated helical carbon nanotube nanocomposites (AuNPs-HCNTs) were fabricated for rutin detection because of its superior sensitivity, the chemical stability of AuNPs, and the superior conductivity and unique 3D–helical structure of helical carbon nanotubes. Results showed the prepared nanocomposites exhibited superior electrocatalytic activity towards rutin due to the synergetic effects of AuNPs and HCNTs. Under the optimized conditions, the developed sensor exhibited a linear response range from 0.1 to 31 μmol/L for rutin with a low detectable limit of 81 nmol/L. The proposed method might offer a possibility for electrochemical analysis of rutin in Chinese medical analysis or serum monitoring owing to its low cost, simplicity, high sensitivity, good stability, and few interferences against common coexisting ions in real samples.

Keywords Nanocomposites · Rutin detection · Helical carbon nanotubes · Au nanoparticles

H. Yang · R. Xing (✉) · S. Liu (✉)
Henan Key Laboratory of Polyoxometalate Chemistry, Institute of Molecular and Crystal Engineering, College of Chemistry and Chemical Engineering, Henan University, Kaifeng, Henan 475004, People's Republic of China
e-mail: xingenjoy@163.com
e-mail: shanhuliu@henu.edu.cn

H. Yang · B. Li · S. Liu
Henan Joint International Research Laboratory of Environmental Pollution Control Materials, College of Chemistry and Chemical Engineering, Henan University, Kaifeng, Henan 475004, People's Republic of China

R. Cui
Jiangsu Laboratory of Advanced Functional Materials, Department of Chemistry and Materials Engineering, Changshu Institute of Technology, Changshu 215500, China

Introduction

Flavonoids are considered versatile components in many drugs and plants with multiple health benefits. One of the most abundant flavonoids, rutin (3′, 4′, 5, 7-tetrahydroxy flavone 3β-drutinoside), has many properties and functions such as antihypertensive, anti-inflammatory, antibacterial, anti-aging, and antioxidant, which has been used clinically as a therapeutical drug worldwide (Ahmad et al. 2016; Ismail et al. 2016). Therefore, it is of great importance to find a sensitive analytical approach for rutin determination in drugs and plants.

To date, various analytical methods have been developed for the determination of rutin, such as high performance liquid chromatography (Ibrahim et al. 2016), spectrophotometric analysis (Chen et al. 2012; Soares et al. 2015), capillary electrophoresis analysis (Li et al. 2002; Wang et al. 2003), flow injection chemiluminescence (Yang et al. 2010a), and so on. However, some of these methods often require complicated pre-concentration

procedures and expensive instruments with mass use of organic solvents, which hamper their "in situ" application and make them inconvenient in practice. The demand for rapid and sensitive detection of flavonoid compounds has been met by electrochemical method with the merits of simplicity, sensitivity, stability, and the possibility to construct portable devices for on-site determination, more importantly the inherent redox properties of rutin (Zhan et al. 2010; Pang et al. 2015).

In the electrochemical procedure, the crucial step is to fabricate suitable modified electrodes using superior sensing materials to improve the electrochemical behaviors of analytes, such as sensitivity, stability, and antifouling ability. Different kinds of nanomaterials including metal nanoparticles (Yang et al. 2015; Ensafi et al. 2016; Li et al. 2016; Nguyen et al. 2017), carbon nanotubes (Bagheri et al. 2016; Xing et al. 2017; Yang et al. 2017), graphene oxide (Dai et al. 2016), and zinc oxide nanoparticles (Ghaedi et al. 2016) have been proven to be superior carriers to enhance response signals. For example, Zou et al. prepared an Au–Ag nanoring/NG-modified electrode to detect rutin (Zou et al. 2016) and Yang et al. investigated the electrochemical behavior of rutin on a gold nanoparticle/ethylenediamine/multi-wall carbon nanotube-modified glassy carbon electrode (AuNPs/en/MWNTs/GCE) (Yang et al. 2010b). Both of them exhibited good detection range and lower detection limit, to obtain the material which had better performance and simple preparation. Helical carbon nanotubes (HCNTs) with a particular 3D–helical structure attracted intense interest in micromagnetic sensors, mechanical microsprings and actuators, high elastic electroconductors, and so forth. In our previous report, HCNTS were proved to possess outstanding peroxidase catalytic activity and electrocatalytic activity (Cui et al. 2011b, 2012). Herein, for the first time, AuNPs-HCNTs were developed through simple electrostatic interactions and used for rutin detection because of its superior sensitivity and chemical stability of AuNPs and the superior conductivity and unique 3D–helical structure of HCNTs. Under the optimized conditions, the developed sensor exhibited a linear response range from 0.1 to 31 μmol/L for rutin with a low detectable limit of 81 nmol/L. The proposed method might offer a possibility for electrochemical analysis of rutin in Chinese medical analysis or serum monitoring owing to its low cost, simplicity, high sensitivity, good stability, and few interferences against common coexisting ions in real samples.

Experimental

Materials

Rutin was obtained from Dalian Meilun Biology Technology Co., Ltd. Phosphate buffer solution was prepared by NaH_2PO_4–Na_2HPO_4 and pH value was adjusted by NaOH and H_3PO_4. Poly(diallyldimethylammonium chloride) (PDDA, Mw = 200,000–350,000) was bought from Sigma. Na_2SO_4, $NaCO_3$, NH_4NO_3, KH_2PO_4, $NaHCO_3$, KCl, $MgSO_4$, glucose, sucrose, uric acid and ethanol were all of analytical reagent grade and purchased from Sinopharm Chemical Reagent Co., Ltd.

Preparation of AuNPs-PDDA-HCNTs

Typical synthesis of HCNTs

HCNTs were synthesized according to our previous literature (Cui et al. 2011a). In brief, HCNTs were prepared by the pyrolysis of acetylene over Fe nanoparticles generated through a combined sol–gel/reduction method at 475 °C.

Preparation of PDDA-HCNTs

The cationic polyelectrolyte PDDA was used to noncovalently functionalize HCNTs in order to increase the solubility to extend the application in electrochemical sensing. In brief, HCNTs were functionalized with PDDA according to the following procedures: 5 mg/mL HCNTs were dispersed into a 0.1% PDDA aqueous solution containing 0.5 M NaCl and the resulting dispersion was sonicated for 30 min to give a homogeneous black suspension. Residual PDDA polymer was removed by centrifugation and the complex was rinsed with water for at least three times. The collected PDDA-HCNTs were redispersed in water with mild sonication to produce a stable solution, which was sonicated for 5 min immediately before preparing the Au-PDDA-HCNTs. For comparison, PDDA-CNTs were also obtained. In brief, CNTs were firstly treated with nitric acid to obtain the carboxylated CNTs. The carboxylated CNTs were separated by centrifugation and were repeatedly washed with double-distilled water until the pH of the carboxylated CNT solution became neutral. Finally, the carboxylated CNTs were treated with PDDA according to the similar procedure as HCNTs.

Preparation of AuNPs

The negatively charged colloidal gold was produced by reduction of gold chloride with sodium citrate. In brief, 100 mL of chloroauric acid solution (containing 0.01% of Au) was heated to the boiling point and 2 mL of sodium citrate solution (1%) was added to the boiling solution with constant stirring. Just in a while, the solution color changed from bright yellow to grayish, to black, and finally to wine red during 2~3 min. Fifteen minutes later, the as-prepared solution was stopped heating, cooled down, and added with double-distilled water until the whole volume was 100 mL.

Preparation of AuNPs-PDDA-HCNTs

PDDA-HCNTs solution (1 mg/mL) was mixed with 50 mL of colloidal gold solution. Once these two solutions were mixed and sonicated, the positively charged PDDA-HCNTs interacted with the negatively charged colloidal gold through electrostatic interactions to fulfill the immobilization of AuNPs on PDDA-HCNTs.

Fabrication of electrochemical sensor

Before the start of the electrochemical experiments and modification procedures, the glass carbon electrode (GCE) was polished to a mirror-like surface with 0.05-mm alumina slurries and ultrasonicated for 3 min in nitric acid (1:1), ethanol, and redistilled water successively. Then, the surface of electrodes was dried by nitrogen. Finally, 10 μL of the as-prepared Au-PDDA-HCNTs suspension was dropped on the pretreated GCE using micropipette and dried in a desiccator for 2 h at room temperature. The prepared modified electrode was denoted AuNPs-PDDA-HCNTs/GCE. For comparison, 10 μL of HCNT, PDDA-CNT, and PDDA-HCNT solution were dropped on the respective GCEs using the same method to obtain the HCNTs/GCE, PDDA-CNTs/GCE, and PDDA-HCNTs/GCE, respectively.

Real samples analysis

The applicability of the AuNPs-PDDA-HCNTs/GCE was tested with real rutin tablets (20 mg/tablet), which were supplied by Shanxi Yunpeng Pharmaceutical Co. Ltd. The rutin sample solution were prepared as follows: 15 rutin tablets were carefully ground in the triturator, transferred to a 50-mL beaker, heated in water bath at 40 °C, and allowed to cool to ambient temperature and filtered, then the obtained supernatant was diluted to the scale of 50 mL with 60% ethanol. A 55.38 μL solution was further diluted with 50 mL of phosphate buffer solution (PBS) (pH 6.0) and then detected by the experimental procedure.

Characterization

CHI660D electrochemical workstation (Shanghai Chenhua Instrument Co., Ltd., Shanghai, China) was employed for all the voltammetric measurement, and HJ-6 magnetic stirring apparatus was used to prepare all the solutions. A conventional three-electrode system was used, including modified GCE as the working electrode, a saturated Ag/AgCl electrode as the reference electrode, and a platinum wire electrode as the auxiliary electrode. The as-synthesized samples were examined by X-ray powder diffraction (XRD), which was carried out on Bruker D8 Advance. Transmission electron microscope (TEM) samples were prepared by dispersing the AuNPs-PDDA-HCNTs in diluted ethanol and then the suspension was deposited onto copper grids, and the morphology was observed on a JEM 2100 transmission electron microscope (JEOL, Tokyo, Japan) with an acceleration voltage of 200 kV. X-ray photoelectron spectroscopy (XPS) was performed using Thermo Scientific escalab 250Xi equipped with Al Ka (hv = 1486.6 eV) at a power of 150 W. To compensate for surface charge effects, binding energies were calibrated using C_{1s} peak at 284.8 eV.

Results and discussion

Characteristics of AuNPs-PDDA-HCNTs

The XRD patterns of PDDA-HCNTs and AuNPs-PDDA-HCNTs were shown in Fig. 1a. In addition to the characteristic reflections of the carbon phase (002) at 25.7°, the characteristic reflections of the gold phase were also observed for Au-PDDA-HCNTs. All the reflections at 38.2°, 44.4°, 64.6°, and 77.6° could be indexed as (111), (200), (220), and (311) lattice planes of Au, respectively, which matched well with the standard pattern (JCPDS Card No. 65-8601). However, the diffraction peaks are relatively broad because of the nanocrystal structure of AuNPs (Rakhi et al. 2009). Figure 1b shows a typical SEM image of AuNPs-
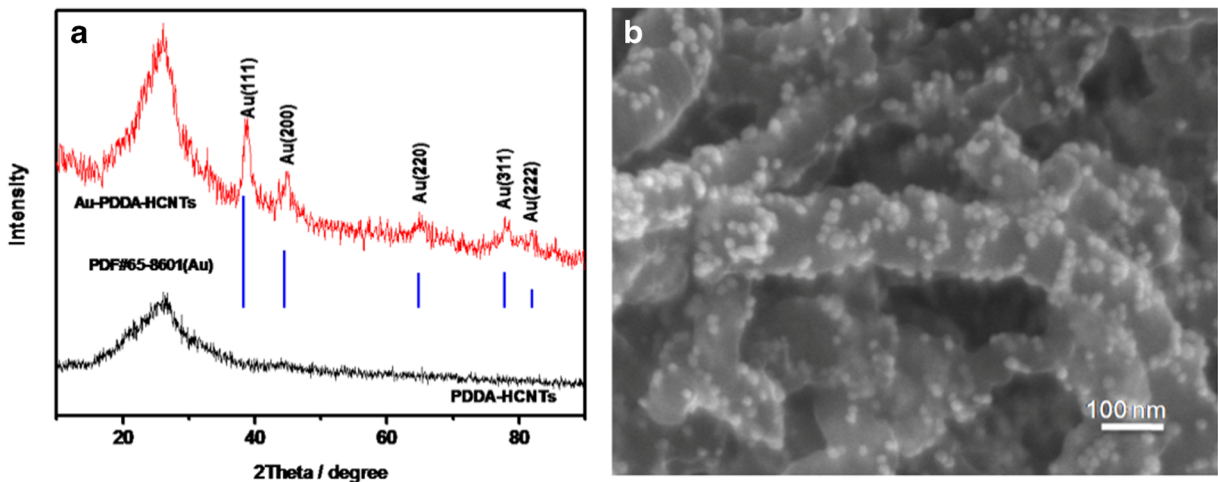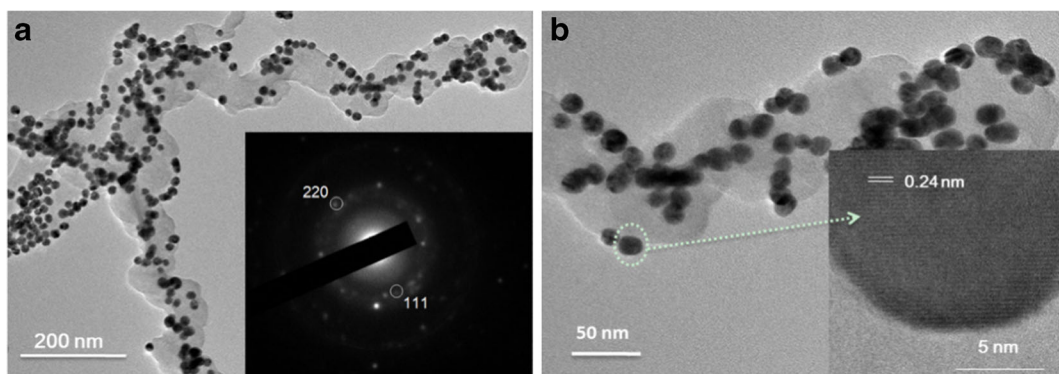
**Fig. 1** **a** XRD patterns of PDDA-HCNTs and AuNPs-PDDA-HCNTs. **b** SEM image of AuNPs-PDDA-HCNTs

PDDA-HCNTs. The basic carbon frame of HCNTs was clearly observed with diameters of about 100 nm and was unchanged after the immobilization of AuNPs (Lee and Kim 2016); most tubes were coiled in a regular and tight fashion with a very short coil pitch. Besides, there were numerous individual nanodots (ca. 13 nm) spreading along the tubes, indicating AuNPs were successfully decorated on the surface of the tubes.

The corresponding SAED patterns (inset in the left of panel Fig. 2a) exhibited additional diffraction dots except diffraction rings, which can be assigned to the (220) and (111) planes of gold nanocrystals. More evidence on the assembly of AuNPs was obtained from high-resolution TEM observation (Fig. 2b). AuNPs display high crystallinity with clear lattice fringes. The experimental lattice spacing of 0.24 nm is analogous to the (111) planes of AuNPs.

Moreover, the incorporation of AuNPs on HCNTs was further demonstrated by XPS measurements (Fig. 3), which is considered as a powerful tool for identifying the chemical compositions and oxidation states of the surface of nanocomposites. As shown in Fig. 3a, compared with that of HCNTs, the XPS spectrum of PDDA-HCNTs shows a slight N1s peak at 380 eV, which illustrated that PDDA was absorbed on the surface of HCNTs. In the XPS spectrum of AuNPs-PDDA-HCNTs, the photoelectron peak of Au4f appeared at 85 eV beside the photoelectron peaks of C1s, N1s and O1s. In the close-up view of the Au4f region, Au4f had binding energy values of 84.0 and 87.8 eV for 4f7/2 and 4f5/2, respectively. These values are close to the typical values for Au^0 that were reported previously (Jaramillo et al. 2003). These above results indicated that followed by the functionalization of PDDA and the

Fig. 2 **a** TEM image of AuNPs-PDDA-HCNTs, inset in the panel (**a**) shows the SAED pattern. **b** Enlarged TEM for Au-PDDA-HCNTs, inset in panel (**b**) shows HRTEM image of one AuNP
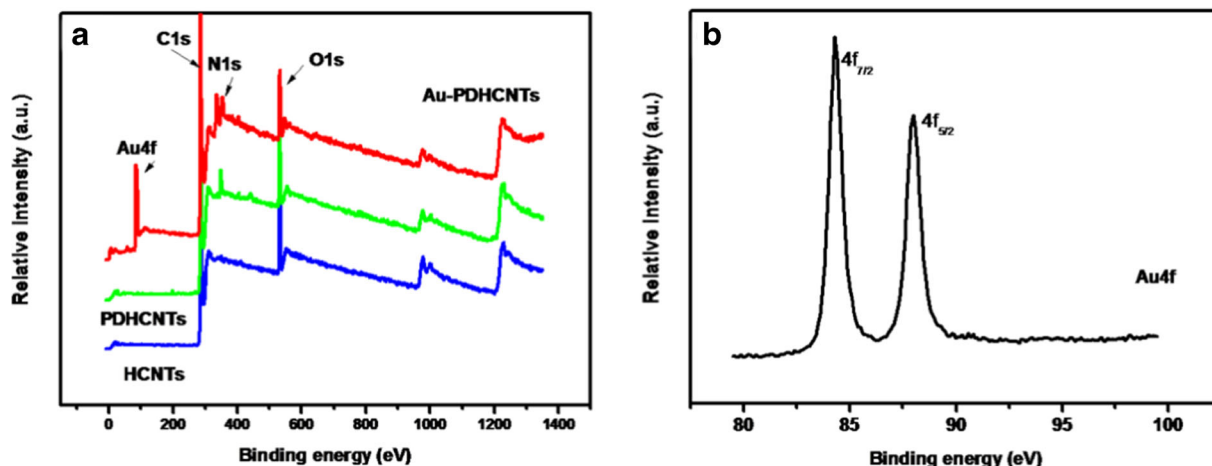
Fig. 3 **a** XPS spectra of HCNTs, PDDA-HCNTs, and AuNPs-PDDA-HCNTs. **b** Au4f high resolution XPS spectra of AuNPs-PDDA-HCNTs

loading of AuNPs, AuNP-PDDA-HCNT nanocomposites were obtained and AuNPs were successfully immobilized on the outer surface of the nanocomposites in a well-dispersed way. It is reported that gold nanoparticles could be employed for improving the biocompatibility and active reaction site and thus for increasing the detection performance (Liu et al. 2012; Lu et al. 2013).

As we all know, electrochemical impedance spectroscopy (EIS) is a powerful tool for investigating the interface features of surface-modified electrodes. The typical Nyquist plot of EIS includes a semicircle at higher frequencies and a linear portion at lower frequencies, which correspond to the electron transfer-limited process and the diffusion-limited process, respectively. Figure S1 shows the impedance plots of AuNPs-PDDA-HCNTs/GCE and bare GCE in 0.1 mol/L KCl solution containing 5 mmol/L $K_3[Fe(CN)_6]$/5 mmol/L $K_4[Fe(CN)_6]$. A remarkable decrease in the semicircle diameter was observed using AuNPs-PDDA-HCNTs/GCE compared to bare GCE, possibly resulting from the facilitated electron transfer based on AuNP-PDDA-HCNT composites. Hence, it can be concluded that AuNPs-PDDA-HCNTs/GCE was a superior electric conducting material and greatly accelerated the electron transfer (Cui et al. 2011a).
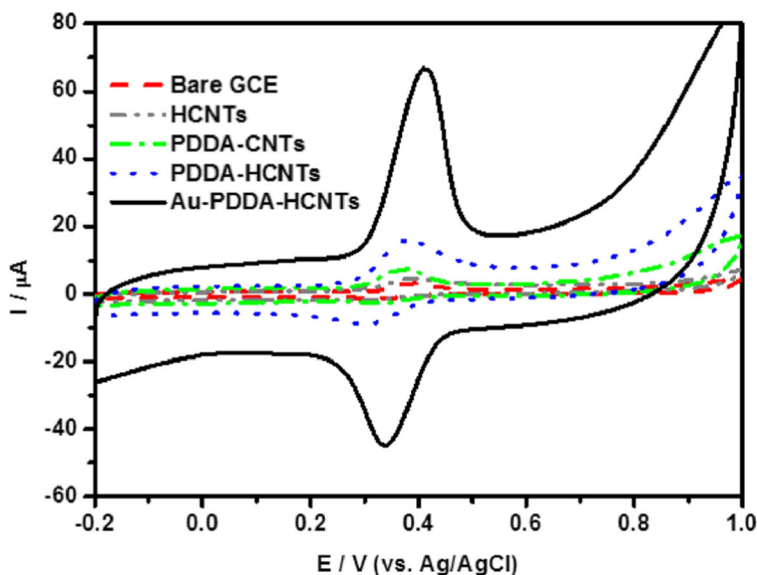
Electrochemical response of rutin
on AuNPs-PDDA-HCNTs/GCE

The electrochemical behavior of rutin (0.1 mM) was studied by cyclic voltammogram (CV) curves on different electrodes such as bare GCE, HCNTs/GCE, PDDA-CNTs/GCE, PDDA-HCNTs/GCE, and AuNPs-PDDA-HCNTs/GCE. As shown in Fig. 4, a pair of redox peaks with different levels appeared on different types of electrodes, indicating that electrochemical reaction of rutin was realized on different electrodes. It should be pointed out that the redox peak currents at the PDDA-HCNTs/GCE were higher than those at bare GCE, HCNTs/GCE, and PDDA-CNTs/GCE, while the pronounced signal enhancement appeared at the AuNPs-PDDA-HCNTs/GCE. The enhancement of the electrocatalytic activity might be attributed to the well-dispersed AuNPs and HCNTs in the nanocomposites and the unique 3D–helical structure of HCNTS.

Figure S2 shows the CVs in the absence (a) and presence (b) of rutin (0.1 mM) on AuNPs-PDDA-HCNTs/GCE. Without rutin, no redox peak was observed. As a comparison, a pair of redox peaks of rutin appeared at + 0.4 V and 0.35 V (vs. Ag/AgCl) in the presence of rutin. These phenomena clearly demonstrated that the improvement of the electrocatalytic activity of the electrode resulted from not only the superior sensitivity and chemical stability of AuNPs but also the superior conductivity and unique 3D–helical structure of HCNTs. So the combination of AuNPs and HCNTs played an important role in facilitating the electron-transfer processes, improving the reversibility and enhancing the sensitivity for rutin. Therefore, an electroanalytical method was developed for the sensitive detection of rutin based on AuNPs-PDDA-HCNTs/GCE and a schematic representation was shown in Scheme 1.

Fig. 4 CVs of 0.1 mM rutin in a 0.1 M PBS solution (PH 6) on different types of electrodes at 50 mV/s

## Optimization of electrode preparation conditions and rutin detection conditions

Effect of solution pH

The effect of solution pH on the electrochemical response of 0.1 mM rutin was investigated when the pH of PBS solution ranged from 2 to 8. As seen clearly in Fig. 5a, the highest oxidation peak appears when the solution pH was 6, and the peak current decreased when the solution pH was higher than 6. Furthermore, the

effect of pH on the electrochemical behaviors of rutin was also investigated and shown in Fig. 5b. It is found that the redox peak potentials shifted to more negative values as the pH increased over a range from 2.0 to 8.0, and the oxidation peak potentials presented a linear relationship with the pH values increased as follows, $E_{pa}/V = 0.729 – 0.0532$ pH ($R^2 = 0.991$) (Fig. 5b). Since E_p can be expressed as (at 25 °C):

$$E_p = E_0 - \frac{m}{n}\ 0.059\ pH$$

Scheme 1 Schematic representation of rutin detection on AuNPs-PDDA-HCNTs/GCE by electrochemical method
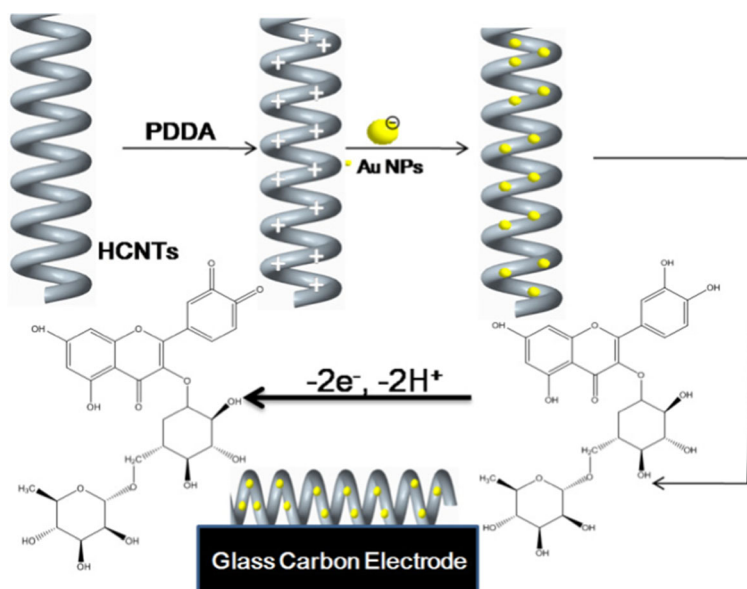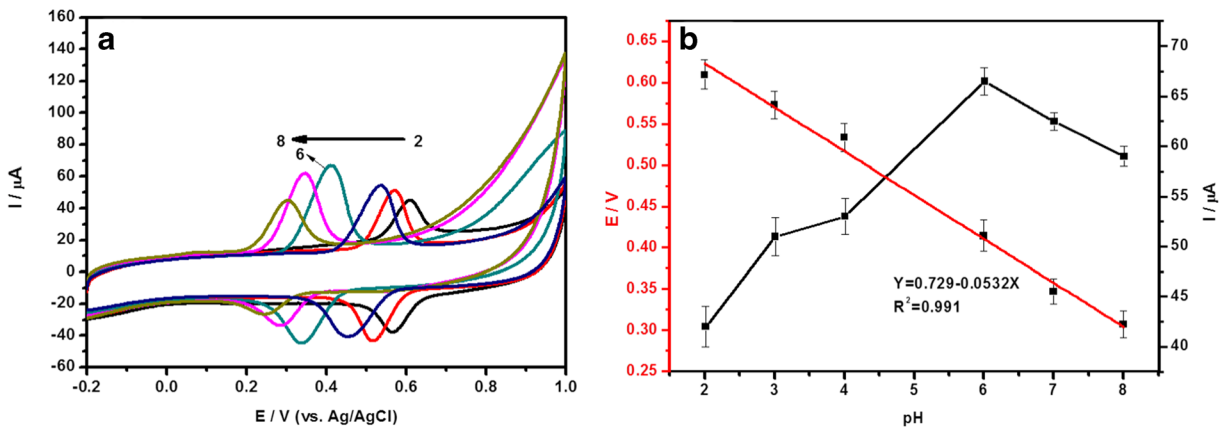
Fig. 5 a: CVs of 0.1 mM rutin on AuNPs-PDDA-HCNTs/GCE in 0.1 M PBS with various pH values (2–8): 2.0, 3.0, 4.0, 6.0, 7.0, and 8.0. b Influence of the pH on the current response and the peak potential of the oxidation of 0.1 mM rutin in 0.1 M PBS on AuNPs-PDDA-HCNTs/GCE

where E_0 is the standard potential, m the number of protons transferred, and the value of m/n was obtained to be one from the slope of the relationship between E_p and pH. This also means that the number of protons involved in the electrode reaction was two, which is well in accordance with the classical electrochemical characteristic of rutin (Zhou et al. 2012). A possible redox mechanism of rutin on the AuNPs-PDDA-HCNTs/GCE was proposed in Scheme 1.
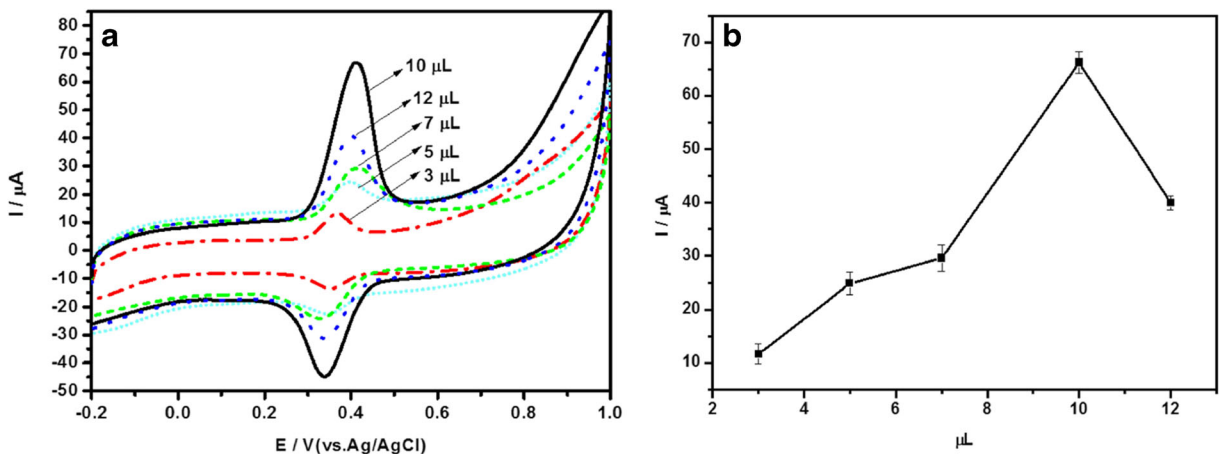
Effect of the deposition amounts of AuNPs-PDDA-HCNTs nanocomposites

The effect of the deposition amount of the nanocomposites on the oxidation peak current of 0.1 mM rutin was also investigated. As seen in Fig. 6, the oxidation peak current increased as the deposition amount increased from 3 to 10 μL; afterwards, the peak current decreased with further increasing of the deposition amount. The reason may be that the insufficient deposition of the nanocomposites led to the incomplete accumulation of rutin in solution, while too many nanocomposites would block the charge transfer between the composites and the solution, which was not favorable to the electrocatalytic oxidation of rutin (An et al. 2013). Thus, 10 μL was selected as the optimal deposition amount in the experiments.

Effect of the scan rates

Figure 7a shows the CVs of 0.1 mM rutin at different scan rates on AuNPs-PDDA-HCNTs/GCE under the

Fig. 6 a CVs of 0.1 mM rutin (pH 6.0) on AuNPs-PDDA-HCNTs/GCE in a 0.1 M PBS with various deposition amounts of the nanocomposites. Scan rate: 50 mVs^{-1}. b The relationship between the peak current I_p and the deposition amount of the nanocomposites
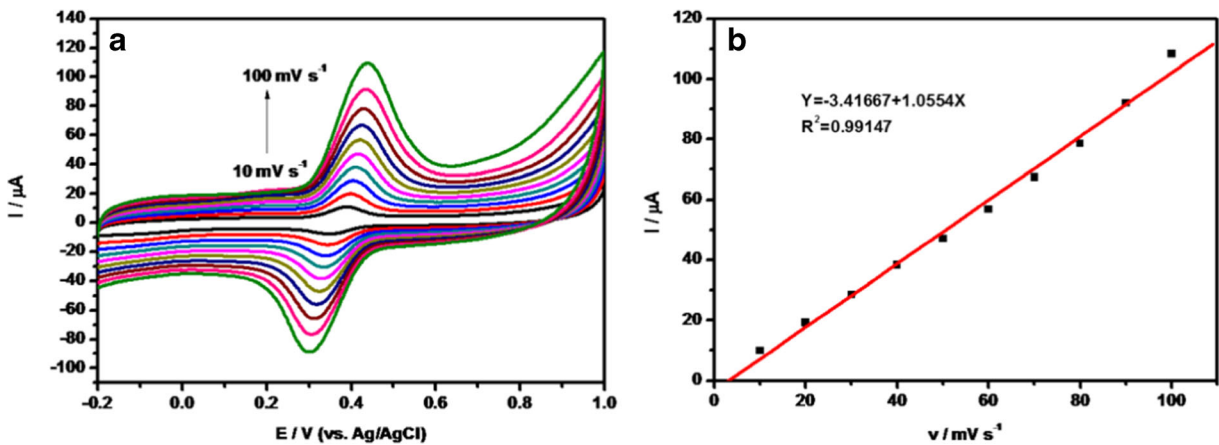
Fig. 7 **a** CV curves of 0.1 mM rutin on AuNPs-PDDA-HCNTs/GCE at different scan rates from 10 to 100 mVs^{-1}. **b** The relationship between the peak currents I_p and the scan rates

optimal conditions. On the modified electrodes, the peak currents increased linearly with increasing the scan rates (Fig. 7b) and shifted slightly towards the positive and negative direction, indicating that the oxidation of rutin on this electrode is surface-controlled not diffusion-controlled (Liu et al. 2013; Madrakian et al. 2014).

Figure 8 shows the CVs of different concentrations of rutin in PBS (0.1 M, pH 6.0) on AuNPs-PDDA-HCNTs/GCE at a scan rate of 100 mV/s. The wave shape of all the curves was similar, but the area of the curves became larger with increasing the concentration of rutin, which suggested that the oxidation peak at about 0.40 V was caused by the oxidation of rutin on AuNPs-PDDA-HCNTs/GCE. The inset of Fig. 8 shows the catalytic

current was proportional to the concentration of rutin within the range from 0 to 70 μM.

Figure 9 displays the i–t plots of successive addition of rutin into a stirring solution of 0.1 M PBS (pH 6.0) at + 0.4 V on AuNPs-PDDA-HCNTs/GCE. The reduction current rapidly increased to reach steady-state value within 3 s after the rutin of certain concentration was added. It may be attributed to the synergistic effect of AuNPs and HCNTs, providing a superior conductive pathway to transfer electrons. As shown in the inset of Fig. 9, the response current was proportional to the concentration of rutin over the range from 0.1 μM to 30 μM with a correlation coefficient of 0.99545. The sensitivity was found to be 1.44 μAμM^{-1} cm^{-2}.

Fig. 8 CV curves of different concentrations of rutin in PBS (0.1 M, pH 6.0) on AuNPs-PDDA-HCNTs/GCE at a scan rate of 100 mV/s
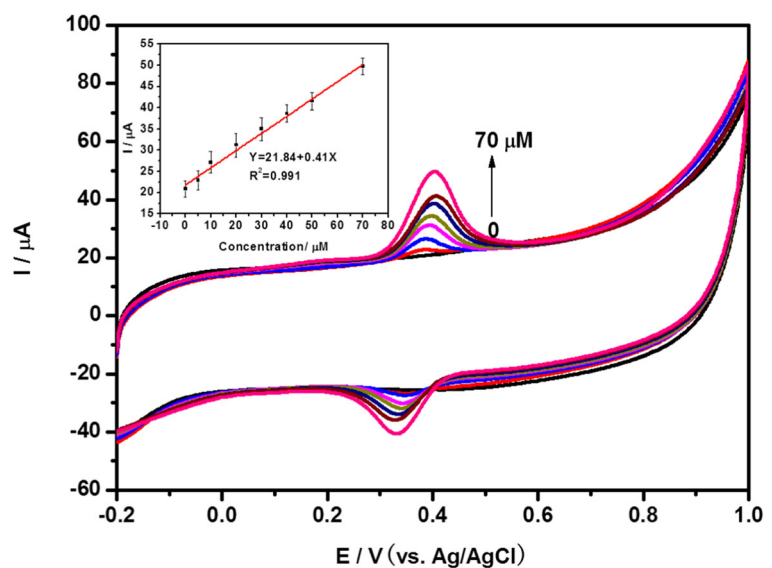
Fig. 9 Amperometric current responses of successive addition of rutin in PBS solution at pH 6.0; working potential: + 0.40 V. Insert: The plot of amperometric current response vs. rutin concentration in the range of 0.1 μM to 30 μM
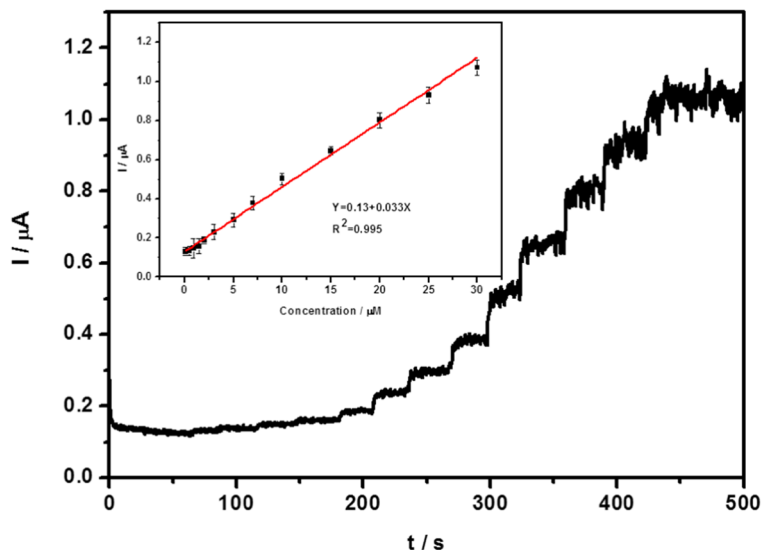
Moreover, the limit of detection (LOD) was 0.081 μM at the signal to noise of 3.

The comparison of the analytical performance of AuNPs-PDDA-HCNTs/GCE with other rutin sensors was presented in Table 1. It can be seen that the fabricated electrode offered a preferable detection limit for rutin compared to the reported literature. The influence of various substances as potentially interfering compounds was studied on the determination of rutin (10 μM) using amperometry. The tolerance limit was defined as the maximum concentration of the interfering substance that caused an error less than ± 5% for the determination of rutin. Most of the inorganic salts did not interfere in the rutin analysis. Moreover, as can be

Table 1 Comparison of AuNPs-PDDA-HCNTs/GCE with other electrodes for rutin determination

Electrode	Detection limit (nM)	Ref.
SWCNT-modified carbon ionic liquid electrode carbon ionic liquid electrode	70	(Zhu et al. 2010)
Pyridinium-based ionic liquid modified carbon paste electrode	358	(Sun et al. 2008)
Ionic liquid modified carbon ceramic electrode	90	(Zhan et al. 2010)
CeO$_2$-modified gold electrode	200	(Wei et al. 2007)
MWNTs/β-cyclodextrin	200	(He et al. 2006)
Au-PDDA-HCNTs/GCE	81	This work

seen in Fig. S3, 4.0 mM of Na$_2$SO$_4$, NaCO$_3$, NH$_4$NO$_3$, KH$_2$PO$_4$, NaHCO$_3$, KCl, MgSO$_4$, glucose, sucrose, uric acid, and ethanol had no significant amperometric responses in the determination of rutin.

The repeatability of AuNPs-PDDA-HCNTs/GCE was examined by measuring the responses of the mixture of 0.10 mM rutin in 0.1 M PBS (pH 6.0) for six successive measurements. Results showed that the relative standard deviation (RSD) was 2.1% for rutin. There was a small decrease in the first three cycles; after that, the peak currents were stable with no shift in potential. Thus, the electrode could be used as a superior electrocatalytic material for sensitive and stable determination of rutin. In addition, more than 93% of its initial current was retained after being stored for a week at room temperature, suggesting the good stability of the modified electrode.

To evaluate the possible applications of the proposed method, AuNPs-PDDA-HCNTs/GCE was used to analyze rutin content in tablet samples. The rutin tablets were obtained from recovery experiments which were carried out by spiking standard rutin solution in the sample containing 10 μM rutin which was extracted above and diluted by 0.1 M PBS (pH 6.0) using the standard addition method. The results were satisfactory with the recovery 99.6–102.1%, which indicated clearly that this method developed in this work was suitable for rutin determination in real samples with high sensitivity and precision (Table 2).

Table 2 Determination of rutin in tablets with the proposed detection strategy ($n = 3$)

No.	Added (μM)	Expected (μM)	Found (μM)	Recovery (%)
1	0	10	10.1	100.1
2	5	15	14.94	99.6
3	10	20	20.42	102.1

Each tablet contains 20 mg

Conclusion

In this paper, a novel electrochemcial sensor based on AuNPs-PDDA-HCNTs nanocomposites was successfully fabricated for the sensitive detection of rutin. Synergy signal amplification effect was observed by the combination of the superior sensitivity and chemical stability of AuNPs and the outstanding conductivity and unique 3D–helical structure of HCNTs during rutin electrochemical redox on the modified electrodes; thus, rutin was successfully determined in real samples. AuNPs-PDDA-HCNTs/ GCE exhibited wider linear range, superior high sensitivity, lower detection limit, and better stability. This study might provide a promising way for the design of novel HCNT devices and superior electrochemical sensors.

References

Ahmad N, Ahmad R, Naqvi AA, Alam MA, Ashafaq M, Samim M, Iqbal Z, Ahmad FJ (2016) Rutin-encapsulated chitosan nanoparticles targeted to the brain in the treatment of cerebral ischemia: rutin-encapsulated chitosan nanoparticles for treatment of cerebral ischemia. Int J Biol Macromol 91:640–655

An J, Bi Y-Y, Yang C-X, Hu F-D, Wang C-M (2013) Electrochemical study and application on rutin at chitosan/ graphene films modified glassy carbon electrode. J Pharm Anal 3:102–108

Bagheri H, Khoshsafar H, Amidi S, Ardakani YH (2016) Fabrication of an electrochemical sensor based on magnetic multi-walled carbon nanotubes for the determination of ciprofloxacin. Anal Methods 8:3383–3390

Chen Z, Qian S, Chen J, Chen X (2012) Highly fluorescent gold nanoclusters based sensor for the detection of quercetin. J Nanopart Res 14:1264

Cui R, Han Z, Pan J, Abdel-Halim ES, Zhu J-J (2011a) Direct electrochemistry of glucose oxidase and biosensing for glucose based on helical carbon nanotubes modified magnetic electrodes. Electrochim Acta 58:179–183

Cui R, Han Z, Zhu JJ (2011b) Helical carbon nanotubes: intrinsic peroxidase catalytic activity and its application for biocatalysis and biosensing. Chem–A Eur J 17:9377–9384

Cui R, Wang X, Zhang G, Wang C (2012) Simultaneous determination of dopamine, ascorbic acid, and uric acid using helical carbon nanotubes modified electrode. Sensors Actuators B Chem 161:1139–1143

Dai H, Wang N, Wang D, Ma H, Lin M (2016) An electrochemical sensor based on phytic acid functionalized polypyrrole/ graphene oxide nanocomposites for simultaneous determination of cd(II) and Pb(II). Chem Eng J 299:150–155

Ensafi AA, Rezaloo F, Rezaei B (2016) Electrochemical sensor based on porous silicon/silver nanocomposite for the determination of hydrogen peroxide. Sensors Actuators B Chem 231:239–244

Ghaedi H, Afkhami A, Madrakian T, Soltani-Felehgari F (2016) Construction of novel sensitive electrochemical sensor for electro-oxidation and determination of citalopram based on zinc oxide nanoparticles and multi-walled carbon nanotubes. Mater Sci Eng C 59:847–854

He J-L, Yang Y, Yang X, Liu Y-L, Liu Z-H, Shen G-L, Yu R-Q (2006) β-Cyclodextrin incorporated carbon nanotube-modified electrode as an electrochemical sensor for rutin. Sensors Actuators B Chem 114:94–100

Ibrahim F, Sharaf El-Din MK, El-Shaheny RN, El-Deen AK, Shimizu K (2016) Simultaneous determination of four vasoactive phytochemicals in different pharmaceutical preparations by a simple HPLC-DAD method. Anal Methods 8: 1858–1866

Ismail H, Shabala L, Tian Y, Jacobsen S-E, Shabala S (2016) Rutin, a flavonoid with antioxidant activity, improves plant salinity tolerance by regulating K+ retention and Na+ exclusion from leaf mesophyll in quinoa and broad beans. Funct Plant Biol 43:75–86

Jaramillo TF, Baeck S-H, Cuenya BR, McFarland EW (2003) Catalytic activity of supported au nanoparticles deposited from block copolymer micelles. J Am Chem Soc 125: 7148–7149

Lee M, Kim D (2016) Non-enzymatic carbohydrates detection based on au modified MWCNT field-effect transistor. Mater Lett 169:257–261

Li X, Zhang Y, Yuan Z (2002) Separation and determination of rutin and quercetin in the flowers ofSophora japonica L. by capillary electrophoresis with electrochemical detection. Chromatographia 55:243–246

Li H, Wang W, Lv Q, Xi G, Bai H, Zhang Q (2016) Disposable paper-based electrochemical sensor based on stacked gold nanoparticles supported carbon nanotubes for the determination of bisphenol a. Electrochem Commun 68:104–107

Liu S, Lu F, Liu Y, Jiang L-P, Zhu J-J (2012) Synthesis, characterization, and electrochemical applications of multifunctional Fe3O4@C–au nanocomposites. J Nanopart Res 15:1–8

Liu M, Deng J, Chen Q, Huang Y, Wang L, Zhao Y, Zhang Y, Li H, Yao S (2013) Sensitive detection of rutin with novel

ferrocene benzyne derivative modified electrodes. Biosens Bioelectron 41:275–281

Lu F, Liu S, Jiang L-P, Zhu J-J (2013) Sonochemical fabrication of CdSexTe1−x/au nanotubes and their potential application in biosensing. J Nanopart Res 15:1–9

Madrakian T, Haghshenas E, Afkhami A (2014) Simultaneous determination of tyrosine, acetaminophen and ascorbic acid using gold nanoparticles/multiwalled carbon nanotube/glassy carbon electrode by differential pulse voltammetric method. Sensors Actuators B Chem 193:451–460

Nguyen TT, Pham HT, Dao KA (2017) The effects of polyvinyl-pyrrolidone and thermal annealing on red shifts for absorption spectra of the nanoparticle au/TiO2 thin film with different au ratios. J Mater Sci Mater Electron 28:2075–2085

Pang P, Li H, Liu Y, Zhang Y, Feng L, Wang H, Wu Z, Yang W (2015) One-pot facile synthesis of platinum nanoparticle decorated reduced graphene oxide composites and their application in electrochemical detection of rutin. Anal Methods 7:3581–3586

Rakhi RB, Sethupathi K, Ramaprabhu S (2009) A glucose biosensor based on deposition of glucose oxidase onto crystalline gold nanoparticle modified carbon nanotube electrode. J Phys Chem B 113:3190–3194

Soares MS, Silva DF d, Forim MR, Silva MF d, Fernandes JB, Vieira PC, Silva DB, Lopes NP, de Carvalho SA, de Souza AA, Machado MA (2015) Quantification and localization of hesperidin and rutin in Citrus Sinensis grafted on C. Limonia after Xylella fastidiosa infection by HPLC-UV and MALDI imaging mass spectrometry. Phytochemistry 115:161–170

Sun W, Yang M, Li Y, Jiang Q, Liu S, Jiao K (2008) Electrochemical behavior and determination of rutin on a pyridinium-based ionic liquid modified carbon paste electrode. J Pharm Biomed Anal 48:1326–1331

Wang Q, Ding F, Li H, He P, Fang Y (2003) Determination of hydrochlorothiazide and rutin in Chinese herb medicines and human urine by capillary zone electrophoresis with amperometric detection. J Pharm Biomed Anal 30:1507–1514

Wei Y, Wang G, Li M, Wang C, Fang B (2007) Determination of rutin using a CeO2 nanoparticle-modified electrode. Microchim Acta 158:269–274

Xing R, Yang H, Li S, Yang J, Zhao X, Wang Q, Liu S, Liu X (2017) A sensitive and reliable rutin electrochemical sensor based on palladium phthalocyanine-MWCNTs-Nafion nanocomposite. J Solid State Electrochem 21:1219–1228

Yang D, Li H, Li Z, Hao Z, Li J (2010a) Determination of rutin by flow injection chemiluminescence method using the reaction of luminol and potassium hexacyanoferrate(III) with the aid of response surface methodology. Luminescence 25:436–444

Yang S, Qu L, Li G, Yang R, Liu C (2010b) Gold nanoparticles/ethylenediamine/carbon nanotube modified glassy carbon electrode as the voltammetric sensor for selective determination of rutin in the presence of ascorbic acid. J Electroanal Chem 645:115–122

Yang J-H, Yang H, Liu S, Mao L (2015) Microwave-assisted synthesis graphite-supported Pd nanoparticles for detection of nitrite. Sensors Actuators B Chem 220:652–658

Yang H, Liu D, Zhao X, Yang J, Chang H-B, Xing R, Liu S (2017) AuPd bimetallic nanoparticles-supported carbon nanotubes for selective detection of dopamine in the presence of ascorbic acid. Anal Methods. https://doi.org/10.1039/C7AY00875A

Zhan T, Sun X, Wang X, Sun W, Hou W (2010) Application of ionic liquid modified carbon ceramic electrode for the sensitive voltammetric detection of rutin. Talanta 82:1853–1857

Zhou J, Zhang K, Liu J, Song G, Ye B (2012) A supersensitive sensor for rutin detection based on multi-walled carbon nanotubes and gold nanoparticles modified carbon paste electrodes. Anal Methods 4:1350

Zhu Z, Sun X, Zhuang X, Zeng Y, Sun W, Huang X (2010) Single-walled carbon nanotubes modified carbon ionic liquid electrode for sensitive electrochemical detection of rutin. Thin Solid Films 519:928–933

Zou C e, Bin D, Yang B, Zhang K, Du Y (2016) Rutin detection using highly electrochemical sensing amplified by an au–Ag nanoring decorated N-doped graphene nanosheet. RSC Adv 6:107851–107858